The FASEB Journal • Research Communication

miR148b is a major coordinator of breast cancer progression in a relapse-associated microRNA signature by targeting ITGA5, ROCK1, PIK3CA, NRAS, and CSF1

Daniela Cimino,[*,†,‡,1] Cristiano De Pittà,[#,1] Francesca Orso,[*,†,‡] Matteo Zampini,[#] Silvia Casara,[#] Elisa Penna,[*,†] Elena Quaglino,[*,§] Marco Forni,[*] Christian Damasco,[*,‖] Eva Pinatel,[*,‖] Riccardo Ponzone,[**] Chiara Romualdi,[#] Cathrin Brisken,[††] Michele De Bortoli,[†,‡] Nicoletta Biglia,[¶] Paolo Provero,[*,‖] Gerolamo Lanfranchi,[#] and Daniela Taverna[*,†,‡,2]

[*]Molecular Biotechnology Center (MBC), [†]Department of Oncological Sciences, [‡]Center for Molecular Systems Biology, [§]Department of Clinical and Biological Sciences, [‖]Department of Genetics, Biology, and Biochemistry, and [¶]Department of Gynecology and Obstetrics, University of Torino, Turin, Italy; [#]Department of Biology and Centro Ricerche Interdepartimentale Biotecnologie Innovative (CRIBI) Biotechnology Center, University of Padova, Padua, Italy; [**]Institute for Cancer Research and Treatment (IRCC), Candiolo, Italy; and [††]National Centers of Competence in Research (NCCR) Molecular Oncology, Institut Suisse de Recherche Expérimentale sur le Cancer (ISREC), School of Life Sciences, École Polytechnique Fédérale de Lausanne (EPFL), Lausanne, Switzerland

ABSTRACT **Breast cancer is often fatal during its metastatic dissemination. To unravel the role of microRNAs (miRs) during malignancy, we analyzed miR expression in 77 primary breast carcinomas and identified 16 relapse-associated miRs that correlate with survival and/or distinguish tumor subtypes in different datasets. Among them, miR-148b, down-regulated in aggressive breast tumors, was found to be a major coordinator of malignancy. In fact, it is able to oppose various steps of tumor progression when overexpressed in cell lines by influencing invasion, survival to anoikis, extravasation, lung metastasis formation, and chemotherapy response. miR-148b controls malignancy by coordinating a novel pathway involving over 130 genes and, in particular, it directly targets players of the integrin signaling, such as ITGA5, ROCK1, PIK3CA/p110α, and NRAS, as well as CSF1, a growth factor for stroma cells. Our findings reveal the importance of the identified 16 miRs for disease outcome predictions and suggest a critical role for miR-148b in the control of breast cancer progression.—Cimino, D., De Pittà, C., Orso, F., Zampini, M., Casara, C., Penna, E., Quaglino, E., Forni, M., Damasco, C., Pinatel, E., Ponzone, R., Romualdi, C., Brisken, C., De Bortoli, M., Biglia, N., Provero, P., Lanfranchi, G., Taverna, D. miR148b is a major coordinator of breast cancer progression in a relapse-associated microRNA signature by targeting ITGA5, ROCK1, PIK3CA, NRAS, and CSF1. *FASEB J.* 27, 1223–1235 (2013). www.fasebj.org**

Key Words: microRNA profiling · malignancy · mammary tumor · integrin signaling · prognosis

BREAST CANCER IS THE MOST common malignancy in women worldwide, often fatal because of metastasis dissemination (1). Clinical and pathological parameters, including tumor size, lymph node involvement, and histological grade and age (2), as well as molecular tumor markers, such as estrogen receptor (ER) and progesterone receptor (PR) or ERBB2, are routinely employed to stratify patients with breast cancer according to risk, assess prognosis, and define appropriate therapies (3). However, since patients with similar combinations of features may often have different clinical outcomes, it is urgent to identify new ways to classify the disease. More recently, protein-coding gene expression profilings have been used to improve tumor classifications (4) and expression of certain gene sets, defined as "signatures," were shown to have a prognostic and/or predictive role for patients (5).

Abbreviations: 3′-UTR, 3′ untranslated region; DFS, disease-free survival; ER, estrogen receptor; FDR, false discovery rate; H&E, hematoxylin and eosin; IPA, Ingenuity Pathway Analysis; miR, microRNA; PCA, principal component analysis; PR, progesterone receptor; SAM, significance analysis of microarray; TMRM, tetramethylrhodamine methyl ester

[1] These authors contributed equally to this work.

[2] Correspondence: MBC and Department Onc. Sci., University of Torino, Via Nizza, 52, 10126 Torino, Italy. E-mail: daniela.taverna@unito.it

doi: 10.1096/fj.12-214692

This article includes supplemental data. Please visit *http://www.fasebj.org* to obtain this information.

MicroRNAs (miRs) are new players involved in the establishment and progression of human tumors that appear to be critical biomarkers of cancer with strong classification power. miRs are a class of small noncoding RNAs that negatively regulate protein-coding gene expression post-transcriptionally by targeting mRNAs, mostly at the 3′ untranslated region (3′-UTR) and triggering either translation repression or RNA degradation (6). Investigations for miR levels in human tumors showed that miR expression is altered in cancer compared to normal tissues, and these changes can help to classify tumors more accurately than mRNA expression profiles according to developmental lineage and differentiation status (7). Recent studies demonstrated that breast cancers can be classified into specific tumor pathological phenotypes (ER, PR, proliferation, stage, metastasis, ERBB2) as well as subtypes (luminal A or B, basal-like, $ERBB2^+$ and normal-like) based on miR expression profiles (8, 9). Thus, it seems essential to combine miR and protein-coding gene expression analyses to obtain information for prognosis and cancer treatment. miRs such as let-7, miR-9, miR-10b, miR-21, miR-31, miR-34, miR-126, miR-146, miR-155, miR-200, miR-214, miR-221/222, miR-373, and 520c have been proven to control tumor dissemination. In fact, alterations of their expression in breast cancer cells profoundly affect tumor dissemination (10–12). In our work, we investigated the relationship between altered miR expression and breast cancer metastasis by analyzing miR levels in a cohort of patients with breast cancer, grouped based on disease relapse. In particular, we investigated the biological function and molecular mechanism of a relapse-associated small noncoding RNA, miR-148b.

MATERIALS AND METHODS

Cell culture

Human MDAMB231, 4175 TGL (13), MCF7, and T47D cells and mouse 4T1 cells were maintained in standard conditions: Dulbecco's modified Eagle's medium containing 10 mM Glutamax and 4.5 mg/ml glucose(DMEM Glutamax; Gibco; Invitrogen Life Technologies, Carlsbad, CA, USA), supplemented with 10% heat-inactivated FCS (Biochrom AG, Berlin, Germany), 1 mM sodium pyruvate, 25 mM HEPES (pH 7.4), and 100 mg/ml gentamicin (all from Gibco).

Patients and samples

Frozen primary invasive ductal breast cancer specimens (77) from 25- to 82-yr-old patients were selected from the Tumor Bank of the Department of Obstetrics and Gynecology, University of Torino (Turin, Italy; primary surgery: 1988–2001) for a retrospective study. There was no distant metastasis at diagnosis (M0). Complete clinical-pathological data were updated by follow-up for ≥72 mo (up to 100 mo). All patients were treated with radical modified mastectomy or quadrantectomy and axillary dissection plus breast irradiation. High-risk node-negative and node-positive patients received adjuvant treatments (generally 6 cycles of CMF: 600 mg/m^2 cyclophosphamide, 40 mg/m^2 metotrexate, 600 mg/m^2 5-fluorouracil), and/or 20 mg tamoxifen daily for 5 yr in ER^+ cases. Patient stage distribution was assessed as prescribed by the Union for International Cancer Control (UICC) clinical staging guidelines, and tumor grading was performed as described previously (14). As normal breast controls, 17 frozen mammoplastic reductions were included in the screening. Appropriate ethical approval was obtained for this study.

Reagents and antibodies

miR precursors and inhibitors

Pre-miR miRNA Precursor Molecules–Negative Control 1, miRNA precursors hsa-miR-148b (PM10264) (000471), hsa-miR-214 (PM12124), Anti-miR miRNA Inhibitor–Negative Control 1, and miRNA inhibitor hsa-miR-148b (AM10264) were from Ambion (Austin, TX, USA).

miR detection

TaqMan miRNA assays hsa-miR-148b (000471), hsa-miR-187 (000487), hsa-miR-365 (001020), hsa-miR-10a (000387), hsa-miR-19a (000395), hsa-miR-342-3p (002260), hsa-miR-214 (002306), hsa-RNU44 (001094), and U6 snRNA (001973) were from Applied Biosystems (Foster City, CA, USA).

ECM

Collagen IV and fibronectin were from Sigma-Aldrich (St. Louis, MO, USA).

Apoptosis reagents

FITC-conjugated annexin V was provided by Boehringer Mannheim (Indianapolis, IN, USA). PE-conjugated annexin V was provided by BD Biosciences (Bedford, MA, USA). Tetramethylrhodamine methyl ester (TMRM) was provided by Molecular Probes (Invitrogen Life Technologies). Paclitaxel (Onco-Tain brand) was from Mayne Pharma (Melbourne, Australia), cisplatin was from Ebewe Italia Srl. (Rome, Italy), and doxorubicin was from Sigma-Aldrich.

RNAi

si ITGA5 (Hs_ITGA5_5 siRNA) and All Stars Negative Control siRNA were purchased from Qiagen (Stanford, CA, USA).

Primary antibodies

Anti-N-RAS mAb F155, anti-hsp90 mAb F-8, anti-ROCK1 pAb H-85, and anti-actin pAb I-19 were from Santa Cruz Biotechnology (Santa Cruz, CA, USA). Anti-PIK3CA (4255) was from Cell Signaling Technology (Danvers, MA, USA). Anti-ITGA5 pAb RM10 was kindly provided by G. Tarone (University of Torino, Turin, Italy; ref. 15). Anti-CSF1 mAb M01-1A9 was from Abnova (Taipei, Taiwan), and anti-α-tubulin mAb B5-1-2 was from Sigma-Aldrich.

Secondary antibodies

Goat anti-mouse and goat anti-rabbit HRP-conjugated IgG were from Santa Cruz Biotechnology. All antibodies were used at the producer's suggested concentrations. Matrigel used for *in vivo* tumor growth experiments (BD Matrigel Basement Membrane Matrix High Concentration) was from BD Biosciences.

Primers

Cloning oligonucleotides employed in this study are listed in **Table 1**. RT-PCR assays (Qiagen) employed in this study are listed in **Table 2**.

Plasmid construction and lentiviral infections

Luciferase reporter vectors containing the partial 3′-UTR of the indicated miR-148b target genes were generated following PCR amplification of the 3′-UTR from human cDNA and cloned into the firefly luciferase reporter pMIR-Report vector (Ambion). When indicated, the 3′-UTRs were mutagenized at miR-148b recognition sites using the QuickChange Site-Directed Mutagenesis kit (Stratagene, Cedar Creek, TX, USA) according to the manufacturer's instructions. The miR-148b sensor was obtained by annealing, purifying, and cloning short oligonucleotides containing 3 perfect miR-148b binding sites into the *Spe*I and *Hind*III sites of the pMIR-Report vector. The human pre-miR-148b sequence (a 306-bp fragment containing the pre-miR sequence) was amplified from genomic DNA (MDAMB231) and cloned into pLemiR-tRFP (Open Biosystems, Huntsville, AL, USA) vector to obtain pLemiR-148b (still containing tRFP) vector. The human pre-miR-187 sequence (a 251-bp fragment containing the pre-miR sequence) was amplified from genomic DNA (MDAMB231) and cloned into pWPT (Addgene, Cambridge, MA, USA) vector to obtain pWPT-miR-187 vector. Stable cell lines were generated by lentiviral infection. Lentiviruses were produced by calcium phosphate transfection of 293T cells with 20 μg of specific vector together with 15 μg packaging (pCMVdR8.74) and 6 μg envelope (pMD2.G-VSVG) plasmids, according to D. Trono's laboratory protocol (École Polytechnique Fédérale de Lausanne, Lausanne, Switzerland; http://tronolab.epfl.ch). Supernatant was harvested 48 h post-transfection, filtered with 0.45-μm filters, diluted, and used to infect 3.5×10^5 cells in 6-well plates, in presence of 8 μg/ml Polybrene (Sigma-Aldrich). ITGA5 overexepression was obtained by transfecting pEGFP-N3-ITGA5 expression vector (plasmid 15238; Addgene; ref. 16).

RNA isolation from tissues or cells

After surgical removal, tumor samples were macrodissected by pathologists, quickly frozen, and stored at −80°C. Total RNA was isolated with Concert cytoplasmic RNA reagent (Invitrogen Life Technologies) from 20 to 50 mg tumor tissues, according to the manufacturer's guidelines. Frozen tumors were then homogenized using a ball mill (MM200; Retsch, Düsseldorf, Germany). The suspension was centrifuged at 14,000 *g* for 5 min at 4°C, and then lysed with 0.1 ml of 10% SDS, followed by 0.3 ml of 5 M sodium chloride and

TABLE 1. *Cloning oligonucleotides employed in this study*

Primer ID	Sequence, 5′ 3′
miR-148b_forw (miR-148b overexpression)	TTTCATAGGCACCACTCACTTTAC
miR-148b_rev (miR-148b overexpression)	CCCTTTCCCCTTACTCTCCA
miR-187_forw (miR-187 overexpression)	GTCGAGTCCCTCAGGACAAG
miR-187_rev (miR-187 overexpression)	TTAGGCTGAACGACACGTAG
miR-148b_sensor_forw (luciferase miR-148b sensor)	CTAGTCCACTGCCTGTCTGTGCCTGCTGTCGTAGGATCTACTG CCTGTCTGTGCCTGCTGTTGGACCTGACACTGCCTGTCTGTGCC TGCTGTCCCA
miR-148b_sensor_rev (luciferase miR-148b sensor)	AGCTTGGGACAGCAGGCACAGACAGGCAGTGTCAGGTCCAACA GCAGGCACAGACAGGCAGTAGATCCTACGACAGCAGGCACAGAC AGGCAGTGGA
ROCK1-3′UTR_forw (ROCK1 3′-UTR cloning)	GCACTAGTGTTCCATCTTCGGACGTTGA
ROCK1-3′UTR_rev (ROCK1 3′-UTR cloning)	ATACGCGTCTTCAACAGACCATGCTCCC
ITGA5-3′UTR_forw (ITGA5 3′-UTR cloning)	ATACTAGTAGGCTGACCGACGACTACTG
ITGA5-3′UTR_rev (ITGA5 3′-UTR cloning)	TAACGCGTTTTTGCATACAAACTGGGAGC
PIK3CA-3′UTR_forw (PIK3CA 3′-UTR cloning)	CTCGACTAGTATGATGCTTGGCTCTGGAAT
PIK3CA-3′UTR_rev (PIK3CA 3′-UTR cloning)	CTCGACGCGTATGCTGTTCATGGATTGTGC
CSF1-3′UTR_forw (CSF1 3′-UTR cloning)	CTCGACTAGTTGGACGCACAGAACAGTCTC
CSF1-3′UTR_rev (CSF1 3′-UTR cloning)	CTCGACGCGTTGTTCAGCAGGCAGGTACAG
NRAS-3′UTR_forw (NRAS 3′-UTR cloning)	CTCGACTAGTTAAGTTTTGTCAGAAAAGAGCCAC
NRAS-3′UTR_rev (NRAS 3′-UTR cloning)	CTCGACGCGTCAAAACAGGCCTCTGGAAAA
ITGA5-3′UTR-mut-site a_forw (ITGA5 3′-UTR mutagenesis)	CTGGGGATCCCTCCCCCCCACGTATTATGAAGGACCCTTGTTTA
ITGA5-3′UTR-mut-site a_rev (ITGA5 3′-UTR mutagenesis)	TAAACAAGGGTCCTTCATAATACGTGGGGGGGAGGGATCCCCAG
ITGA5-3′UTR-mut-site b_forw (ITGA5 3′-UTR mutagenesis)	GGGTTCTGCCTGCCAGCCGTAATTATGCTGCCCCTCATCTC
ITGA5-3′UTR-mut-site b_rev (ITGA5 3′-UTR mutagenesis)	GAGATGAGGGGCAGCATAATTACGGCTGGCAGGCAGAACCC
ROCK1-3′UTR-del_forw (ROCK1 3′-UTR mutagenesis)	CATTAAGTTAACAAACATATAAGAAATGTATGTTTGAAATGTA AATTATTCTTAGAACACTTTC
ROCK1-3′UTR-del_rev (ROCK1 3′-UTR mutagenesis)	GAAAGTGTTCTAAGAATAATTTACATTTCAAACATACATTTCT TATATGTTTGTTAACTTAATG
PIK3CA-3′UTR-mut_forw (PIK3CA 3′-UTR mutagenesis)	GCTCACTCTGGATTCCACACGGTACGGTTAATAACTCTCAGCAGGC
PIK3CA-3′UTR-mut_rev (PIK3CA 3′-UTR mutagenesis)	GCCTGCTGAGAGTTATTAACCGTACCGTGTGGAATCCAGAGTGAGC
NRAS-3′UTR-del_forw (NRAS 3′-UTR mutagenesis)	GCCACTTTCAAGCTGTGACACCCTGGTCCT
NRAS-3′UTR-del_rev (NRAS 3′-UTR mutagenesis)	AGGACCAGGGTGTCACAGCTTGAAAGTGGC
CSF1-3′UTR-del-site a_forw (CSF1 3′-UTR mutagenesis)	GACCTGCTGGTCTGTGACAGCCTGAAGG
CSF1-3′UTR-del-site a_rev (CSF1 3′-UTR mutagenesis)	CCTTCAGGCTGTCACAGACCAGCAGGTC
CSF1-3′UTR-del-site b_forw (CSF1 3′-UTR mutagenesis)	CATGAAGGAAGCCATTGTGTGAACACTGTACCTG
CSF1-3′UTR-del-site b_rev (CSF1 3′-UTR mutagenesis)	CAGGTACAGTGTTCACACAATGGCTTCCTTCATG

TABLE 2. *RT-PCR assays employed in this study*

Primer ID	Assay ID
COPZ1	QT00087024
CSF1	QT00035224
CTSA	QT00087381
CXCL5	QT00203686
DYRK2	QT01011073
GRB2	QT00065289
ITGA5	QT00080871
MMP15	QT00014063
NRAS	QT00076874
NRP1	QT00023009
PIK3CA	QT00014861
ROCK1	QT00034972
RRN18S	QT00199367

0.2 ml of chloroform per milliliter of reagent. The lysate was centrifuged at 14,000 *g* for 15 min at 4°C, and the upper aqueous phase was removed and combined with 0.8 vol of isopropyl alcohol for 10 min at room temperature. Total RNA was recovered by centrifugation, washed with 75% ethanol, and finally dissolved in RNase-free water. Total RNA from normal samples or cells in culture was isolated with TRIzol reagent (Invitrogen Life Technologies). Frozen samples were homogenized using an Ultra Turax T50 Basic homogenizer (Bioclass, Pistoia, Italy) and extracted with an acid-phenol: chloroform solution according to the manufacturer's guidelines. RNA quantitation was performed using the NanoDrop 1000 spectrophotometer (Nanodrop, Wilmington, DE, USA). Total RNA integrity and the percentage content of miRs in each sample were assessed by capillary electrophoresis using the Agilent Bioanalyzer 2100 with the RNA 6000 Nano and the Small RNA Nano LabChips, respectively (Agilent Technologies, Palo Alto, CA, USA). Only total RNA samples with an RNA integrity number (RIN) $\geq$ 6 and $<$30% of small RNAs were used for miR microarray analysis.

miR and gene expression profilings

The miR and protein-coding expression profilings were carried out using the Human MicroRNA Microarray kit (V2, 723 miRs) and the Whole Human Genome Oligo Microarray (~41,000, 60-mer oligonucleotide probes), respectively, both from Agilent Technologies. For miR analysis, total RNA (200 ng) was labeled with pCp-Cy3, according to the Agilent protocol (17), and probes were hybridized at 55°C for 22 h. For protein-coding investigations, total RNA (800 ng) was labeled by the Agilent One-Color Microarray-Based Gene Expression protocol, according to the manufacturer's instructions. The synthesized cDNA was transcribed into cRNA and labeled with Cy3. Labeled cRNA (1.65 μg) was used for hybridization at 65°C for 17 h. Slides were scanned on an Agilent microarray scanner. Raw miR and gene expression data are available in the U.S. National Center for Biotechnology Information Gene Expression Omnibus (GEO) database (GSE26666; http:/www.ncbi.nlm.nih.gov/geo/query/acc.cgi?token_jveltssyquiywvo&acc_GSE26666). Interarray normalization was performed with cyclic Lowess for miRs and with quantile for protein-coding expression profilings (18, 19), and the average of replicates was used. To perform differential gene expression analysis, the level of each miR was calculated as $\log_2$ of tumor sample/mammoplastic reduction median. The identification of differential expression for miRs or protein-coding genes was performed using the 2-class significance analysis of microarray (SAM) algorithm (20). SAM uses a permutation-based multiple testing algorithm and associates a variable false discovery rate (FDR) to the significant genes. FDR refers to the percentage of error that can occur in the identification of the statistically significant differentially expressed genes in multiple comparisons; it can be manually adjusted.

Statistical analysis of miR and gene expression data

For miRs, Feature Extraction software (Agilent Technologies) was used to obtain spot quality measures in order to evaluate the quality and the reliability of the hybridization. In particular, the flag gIsFound (set to 1 if the spot has an intensity value significantly different from the local background, 0 otherwise) was used to filter out unreliable probes: flag equal to 0 will be noted as not available (NA). So, in order to perform a more robust and unbiased statistical analysis, probes with a high proportion of NA values were removed from the dataset. NA (40%) was used as threshold in the filtering process, obtaining a total of 237 available human miRs. Principal component analysis (PCA), cluster analysis, and profile similarity searches were performed with Multi Experiment Viewer 4.5.1 (TMev) of the TM4 Microarray Software Suite (21). All heath maps were obtained by TMeV software using an unsupervised 2-dimensional hierarchical clustering approach with average linkage method and Pearson correlation.

Statistical analyses of biological samples

Data are presented as means ± SEM or SD, and 2-tailed Student's *t* test was used for comparison analysis, with values of $P < 0.05$ considered to be statistically significant. Box and whisker plots were prepared based on Liu (22). The bottom and top of the box are, respectively, the first (bottom) and third (top) quartile; the line in the middle corresponds to the median, and circles label outliers.

Statistics for survival analysis

Survival association analyses were performed using the SPSS 18.0 statistical software (SPSS Inc., Chicago, IL, USA) and the Bioconductor suite of software tools (http://www.bioconductor.org). The receiver operating characteristic (ROC) method (23) was used to categorize samples according to miR or mRNA expression. Kaplan-Meier survival curves were used to estimate time-to-event models in the presence of censored cases. Risk differences between the two groups were assessed using the Mantel-Haenszel log-rank test (24). Survival analysis was carried out in both univariate and multivariate setting using Cox's proportional hazard model (25). ITGA5 survival association was evaluated in GSE2034 (26); gene expression values were calculated as described previously (27), and results were divided into two categories according to gene expression levels.

Analysis of human breast cancer data sets

Blenkiron *et al.* (8) and Enerly *et al.* (9) miR expression values and sample phenodata were obtained from GSE7842 and GSE19536, respectively, and from the supplemental materials of the publications.

Target prediction and pathway analysis

The TargetScan 5.1 algorithm (28) was used to predict miR targets. The Ingenuity Pathways Knowledge Base (http://www.ingenuity.com) is currently the world's largest database of knowledge on biological networks, with annotations orga-

nized by experts. We exploited this database to look for enrichments in specific pathways among the relapse (or other category)-associated miR putative targets. Enrichment significance in pathways analysis is shown as the negative $\log_{10}$ of the *P* value. The *P* value is calculated with the right-tailed Fisher's exact test. Ingenuity networks are scored based on the number of network eligible molecules they contain. The network score is based on the hypergeometric distribution and is calculated with the right-tailed Fisher's exact test. The score is the negative log of this *P* value.

Additional cell transfections and infections, qRT-PCRs, apoptosis, luciferase assays, protein preparation, immunoblotting, and i*n vitro* and *in vivo* biological studies were all performed as indicated in detail in Penna *et al.* (12).

RESULTS

Sixteen relapse-associated miRs classify breast tumors

In a retrospective study, we analyzed miR expression in 77 primary human breast ductal tumors as well as 17 mammoplastic reductions (**Table 3**), using microarrays (a 723-miR platform) and a 2-class SAM. In particular, when we compared patients with relapse ($n=41$) or without relapse ($n=36$), within ≥72 mo from surgery, 16 differentially expressed miRs were identified and expressed as fold changes or levels, relative to the median of the healthy controls, $\log_2$ tumors/controls (**Fig. 1**). Within relapsing/nonrelapsing patients, validation of microarray data was performed by qRT-PCR analysis for miR-148b, miR-365, and miR-10a using $n = 10$/group (not shown). By using the 16 relapse-associated miRs together as a whole (as a group), we identified two groups of patients with different overall survival (OS; $P=0.018$) and disease-free survival (DFS; $P=0.016$), independent of the lymph node status (Cox proportional-hazards regression model; $P=0.015$) in our study. The same was found when certain individual specific miRs were used, for instance, miR-148b, downregulated in relapsing tumors (OS, $P=0.027$; DFS, $P=0.036$). However, a correlation with survival was not found when our 16 relapse-associated miRs were used as a whole for two other available public datasets (8, 9). These studies refer to ~100 patients each; the primary tumors were used to measure mRNA and miR expression with the goal of identifying tumor subtypes. Notably, in these datasets, our group of 16 relapse-associated miRs could identify tumor subtypes and separate more aggressive (ERBB2$^+$ or basal-like) *vs.* less aggressive (luminal A/B) cancers (Fig. 1*C*, compare solid *vs.* shaded symbols), based on the breast cancer classification in Sorlie *et al.* (4). Moreover, our 16-miR signature could also predict survival, in our cohort, when only luminal tumors ($n=53$) were considered (DFS, $P=0.0097$). In addition, some of the 16 miRs, such as miR10a, miR-101, miR-142-5p, miR-148b, miR-342-3p, miR-342-5p, miR-365, and miR-551b, could distinguish tumor subtypes individually (8, 9 and data not shown). In summary, we identified 16 relapse-associated miRs that could be used in the clinics to identify tumor subtypes and to predict disease outcome.

TABLE 3. *Clinical characteristics of the patients: summary*

Characteristic	Value	%
Tumor samples		
Patients (*n*)	77	
Age (yr)		
Median	54	
Range	25–82	
Tumor stage (*n*)		
1	20	26.0
2	51	66.2
3	3	3.9
4	3	3.9
Tumor grade (*n*)		
1	4	5.2
2	35	45.4
3	33	42.8
Unknown	5	6.5
LN (*n*)		
Positive	44	57.1
Negative	33	42.9
ER (*n*)[a]		
Positive	53	68.8
Negative	24	31.2
PR (*n*)[a]		
Positive	42	54.5
Negative	35	45.4
Subtype (*n*)[b]		
Luminal	53	68.0
ERBB2[b]	14	18.0
Basal	10	12.0
Relapse, ≥72 mo (*n*)		
Yes	41	53.2
ER$^+$	25	61[c]
ER$^-$	16	39[c]
No	36	46.7
ER$^+$	28	78[c]
ER$^-$	8	22[c]
Normal samples		
Patients (*n*)	17	
Age (yr)	13	
Median	43	
Range	20–67	

n, number; LN, lymph node status; ER, estrogen receptor status; PR, progesterone receptor status. [a]ER and PR are defined positive when tumors contain >10 fmol receptors/mg proteins or <10% positive tumor cells. [b]Samples were classified according to ERBB2 mRNA level combined to ER and PR status. [c]Percentage refers to the total of relapsing or nonrelapsing samples.

miR-148b impairs tumor growth and suppresses metastasis formation by altering extravasation and survival

A detailed bioinformatics analysis was carried out for the putative targets of the 16 relapse-associated miRs, as predicted by TargetScan 5.1, using Ingenuity Pathway Analysis (IPA) in order to identify pathways and functions in which each miR was involved. This analysis, together with literature searches, let us to conclude that miR-148b has the potential to coordinate a very high number of pathways relevant for breast cancer and that its function has still to be elucidated. With this in mind, we investigated the biological role of miR-148b in

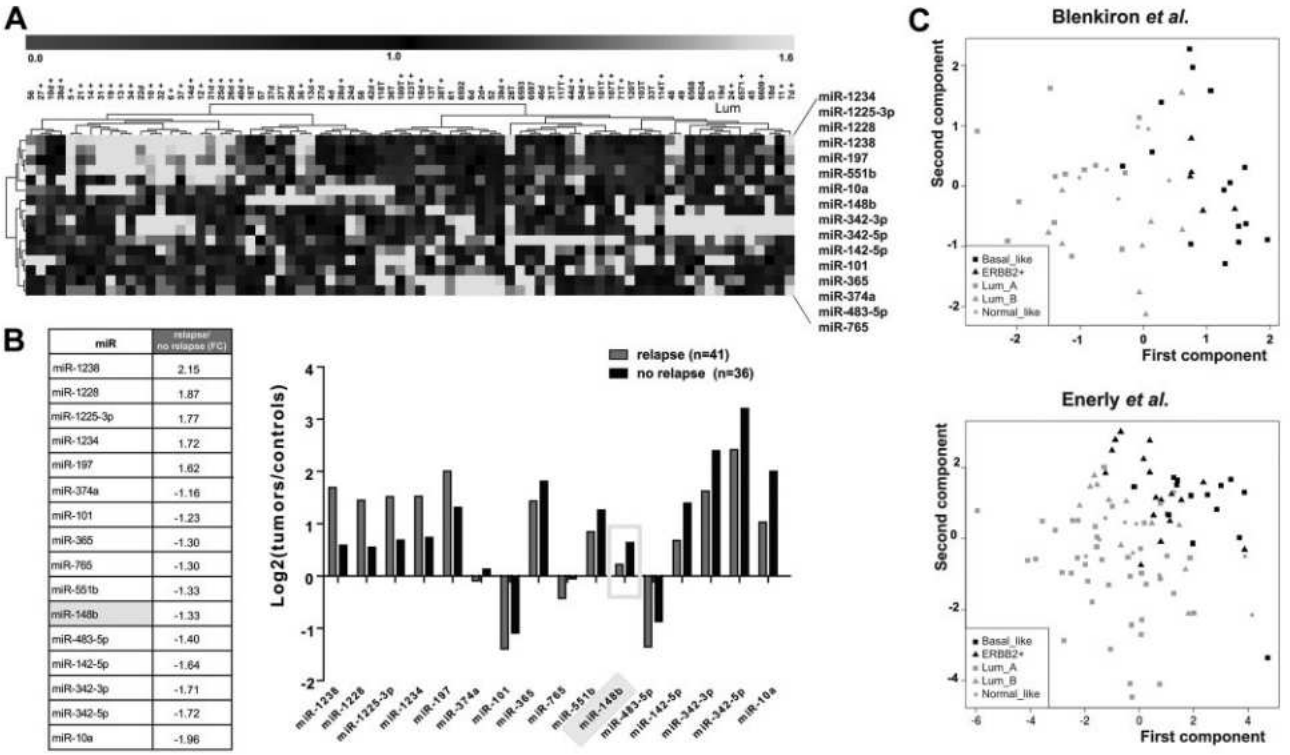

miR	relapse/ no relapse (FC)
miR-1238	2.15
miR-1228	1.87
miR-1225-3p	1.77
miR-1234	1.72
miR-197	1.62
miR-374a	-1.16
miR-101	-1.23
miR-365	-1.30
miR-765	-1.30
miR-551b	-1.33
miR-148b	-1.33
miR-483-5p	-1.40
miR-142-5p	-1.64
miR-342-3p	-1.71
miR-342-5p	-1.72
miR-10a	-1.96

Figure 1. Expression of 16 miRs in relapse-positive (R^+) or relapse-negative (R^-) primary cancers and tumor subtype identification. *A*) Clustering (Pearson correlation, average linkage) for the 16 most modulated miRs considering relapsing ($n=41$) *vs.* nonrelapsing ($n=36$) tumors. Heatmap represents relative miR levels with reference to the median expression across all samples; rows: miR; columns: tumors. *B*) Summary (left panel) and graph (right panel) showing the levels of expression of the 16 most modulated miRs, expressed as fold change (FC) of relapsing/nonrelapsing median values (left panel) or averaged levels ($\log_2$) in R^+ or R^- tumor samples *vs.* mammoplastic reductions (controls). Two-class SAM, FDR 16%. *C*) PCA plots for tumor subtypes using all 16 miRs in Blenkiron *et al.* (8) and Enerly *et al.* (9) datasets. Basal_like, basal; $ERBB2^+$, ERBB2 positive; Lum_A, luminal A; Lum_B, luminal B; normal_like, normal-like breast cancer.

neoplasia by modulating (up or down) its expression in MDAMB231, 4175TGL, 4T1, T47D, and MCF7 mammary tumor cell lines with a different level of malignancy (independently of ER, PR, and ERBB2 expression) and of miR-148b, as measured by qRT-PCR (Supplemental Fig. S1*A*). Transient modulations were obtained using miR-148b precursors or inhibitors or negative controls (pre-miR-148b, anti-miR-148b, or precontrol or anticontrol) and evaluated 48 or 72 h post-transfection for expression and biology (Supplemental Fig. S1*B, C*). Instead, for stable expression, cells were transduced with pLemiR-empty or pLemiR-148b overexpressing lentivirus vectors and selected with puromycin as pools; expression evaluation is shown in Supplemental Fig. S1*C*.

In vitro proliferation was not affected or only slightly modulated up to 4 d for MDAMB231, 4175TGL, and 4T1 cells in stable or transient conditions (Supplemental Fig. S2A and data not shown). However, tumors derived from transduced pLemiR-148b 4175TGL cells grew significantly less compared to controls (pLemiR-EV) when analyzed up to 12 d following injection in the fat pad of immunocompromised NOD/SCID IL2Rγ^{null} mice (see below). When invasion through fibronectin or Matrigel was evaluated by transwell assays for the same cell lines, reduced cell movement was observed in the presence of miR-148b overexpression compared to controls (Supplemental Fig. S2*B* and data not shown). However, no effect was observed when cells were transduced with pWPT-miR-187 (negative control) lentivirus overexpression vectors compared to controls (pWPT-EV or precontrol; Supplemental Fig. S2*B* and data not shown). Instead, increased cell invasion was observed when miR-214 was overexpressed in these cells (Supplemental Fig. S2*B*, ref. 12, and data not shown). When cell adhesion was investigated, increased adhesion on fibronectin and collagen IV was found for MDAMB231 cells overexpressing miR-148b compared to controls. Conversely, down-modulation of miR-148b in MCF7 and T47D cells led to decreased adhesion (Supplemental Fig. S2*C*).

To study the role of miR-148b in *in vivo* metastasis formation, we injected miR-148b-overexpressing (pre-miR-148b) 4T1 cells into the tail vein of female BALB/c syngeneic mice, and analyzed dissemination in lungs. A significant reduction in the number of lung colonies or area occupied by the lesions was found 5 d postinjection compared with controls, as measured in hematoxylin and eosin (H&E)-stained sections (**Fig. 2***A*). More relevantly, when red fluorescent pLemiR-148b-transduced, 4175TGL cells were injected orthotopically into NOD/SCID/IL2Rγ^{null} mice and primary tumors formed, a striking reduction of malignant cell dissemination from the primary tumors to the lungs was observed com-

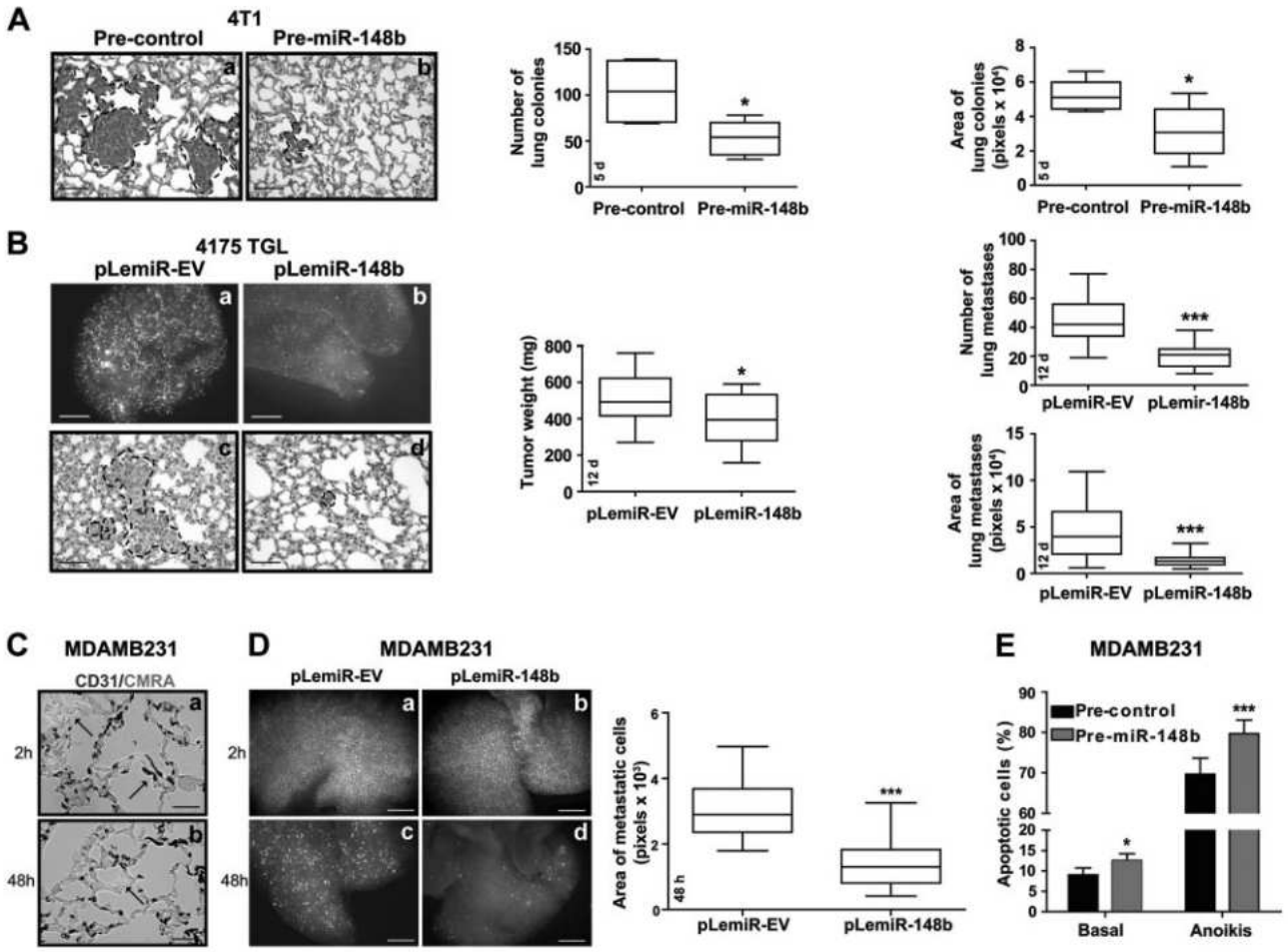

Figure 2. miR-148b impairs metastasis formation in mice by affecting extravasation and survival. *A*) 4T1 cells transiently transfected with negative controls (pre-control; *a*) or miR-148b precursors (pre-miR-148b; *b*) were used to evaluate lung colony formation in BALB/c mice at 5 d after tail vein injection. *B*) Alternatively, 4175TGL cells stably transduced with pLemiR-EV (*a, c*) or pLemiR-148b (*b, d*) overexpression vectors were injected into the mammary gland fat pad of NOD/SCID/IL2Rγ^{null} mice, and primary tumor growth as well as metastasis formation in the lungs were analyzed at 12 d postinjection. *A, B*) Two independent experiments were performed, and results were pooled together (n=10 mice/group) and shown as box and whisker plots for primary tumor weights (*B*) or number (or area) of microscopic colonies (*A*) or metastasis (*B*) in the lungs. Tumor cell dissemination was evaluated in H&E-stained sections at d 5 (*A*) or as fluorescent lesions in the whole lung at d 12 (*B*). Representative H&E stainings are shown. *C, D*) *In vivo* seeding/extravasation assays following tail vein injections in nude mice of red fluorescent MDAMB231 cells, stably transduced with pLemiR-EV or pLemiR-148b overexpression vectors. *C*) Representative fields of lung sections at 2 h (*a*) or 48 h (*b*) postinjection, stained for CD31 (black) and containing red fluorescent MDAMB231 cells (here visible in light gray). No cells were found in the vessels at 48 h. *D*) Left panels: red fluorescent cells in the whole lungs at 2 h (*a, b*) or 48 h (*c, d*) postinjection. Right panel: quantitation of the red fluorescent cells (area) at 48 h for n = 8 mice/group. *E*) MDAMB231 cells transfected with miR-148b precursors or their negative controls (pre-miR-148b or control) were grown in presence or absence (anoikis) of attachment and without serum for 48 h. Percentage of apoptotic cells was evaluated by TMRM and annexinV-FITC staining in a FACS analysis. ^{High}TMRM-^{Low}AnnexinV, healthy cells; ^{Low}TMRM-^{High}AnnexinV, apoptotic cells. Three independent experiments were performed in duplicate; pooled quantitations are shown as means ± SEM. Scale bars = 60 μm (*A*; *Bc, d*); 2 mm (*Ba, b*; *D*); 120 μm (*C*). *$P < 0.05$; **$P < 0.01$; ***$P < 0.001$.

pared to controls (Fig. 2*B*). Quantitations refer to the red fluorescent metastatic foci (number/area) in the lungs at 12 d postinjection (Fig. 2*B*); H&E sections are shown (Fig. 2*B*). Similar results were obtained with pLemiR-148b-transduced 4T1 cells (not shown). Notably, when similar experiments were previously performed with miR-214-overexpressing 4T1 cells, increased dissemination was observed (12).

Based on this, we assessed the involvement of miR-148b in extravasation and survival in the blood circulation, two essential steps of the metastatic dissemination. To investigate extravasation *in vivo*, red fluorescent pLemiR-148b-transduced MDAMB231 cells were injected into the tail vein of immunocompromised mice, and cell seeding and extravasation in the lung were evaluated at 2 or 48 h postinjection. A high percentage of cells lodged in the lung at 2 h (within the vessels or outside) in the presence or absence of miR-148b. However, extravasation was highly reduced for miR-148b-overexpressing cells compared to controls, as quantitation of the area occupied by metastatic cells showed (Fig. 2*C, D*). Vessels were labeled for CD31

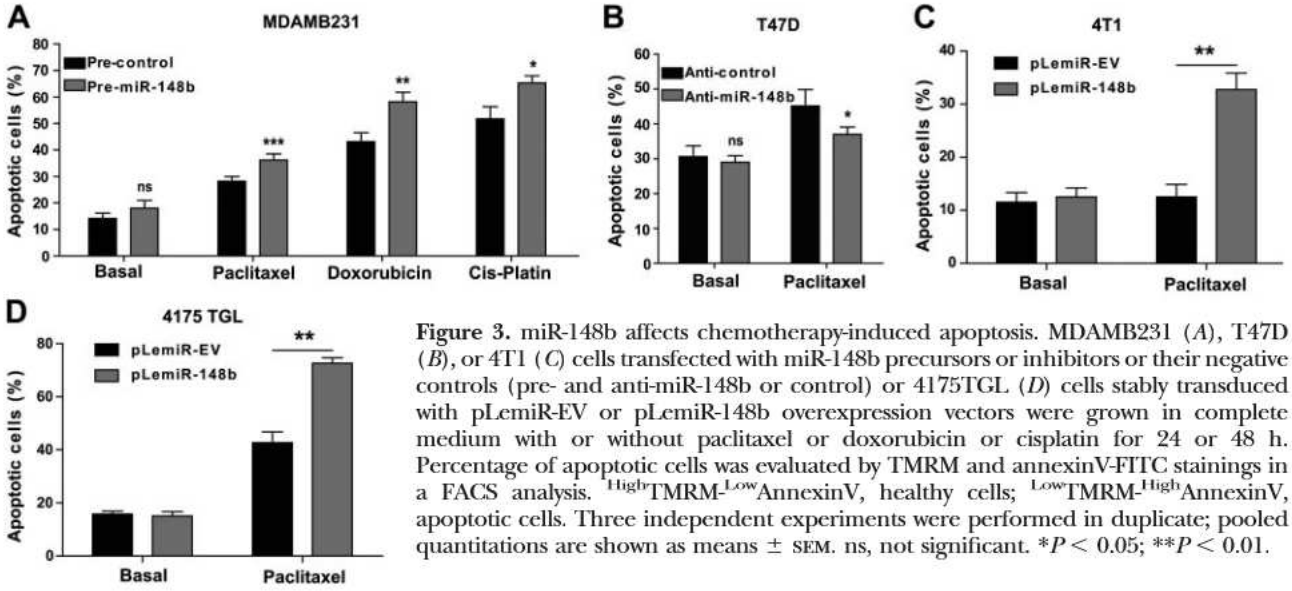

Figure 3. miR-148b affects chemotherapy-induced apoptosis. MDAMB231 (*A*), T47D (*B*), or 4T1 (*C*) cells transfected with miR-148b precursors or inhibitors or their negative controls (pre- and anti-miR-148b or control) or 4175TGL (*D*) cells stably transduced with pLemiR-EV or pLemiR-148b overexpression vectors were grown in complete medium with or without paclitaxel or doxorubicin or cisplatin for 24 or 48 h. Percentage of apoptotic cells was evaluated by TMRM and annexinV-FITC stainings in a FACS analysis. ^{High}TMRM-^{Low}AnnexinV, healthy cells; ^{Low}TMRM-^{High}AnnexinV, apoptotic cells. Three independent experiments were performed in duplicate; pooled quantitations are shown as means ± SEM. ns, not significant. $*P < 0.05$; $**P < 0.01$.

(Fig. 2*C*). To investigate survival in the blood circulation, we evaluated apoptosis in miR-148b-overexpressing MDAMB231 cells kept without serum and with or without (anoikis) adhesion for 48 h by cytofluorimetric analyses, and reduced survival was observed compared to controls (Fig. 2*E*), which suggests a potential role for miR-148b in tumor cell intraluminal viability and initial survival. All these experiments strongly suggest that miR-148b is involved in metastatic cell dissemination by controlling tumor growth and cell survival in anoikis but mostly by inhibiting cell escaping through the endothelial cells of the vessels.

miR-148b expression enhances chemotherapy-induced apoptosis

Considering the relevance of chemotherapy response for tumor progression, we analyzed the response to paclitaxel, doxorubicin, and cisplatin following 24 or 48 h treatment in miR-148b-overexpressing (MDAMB231, 4175TGL, 4T1) or down-modulated (T47D) cells by cytofluorimetric analyses. A significant modulation in cell survival was found for all cell lines and treatments compared to controls (**Fig. 3**), favoring a positive role for miR-148b in chemotherapy response.

miR-148b modulates multiple genes

To identify genes directly or indirectly modulated by miR-148b, miR-148b-overexpressing MDAMB231 cells were first used to perform whole human genome gene expression analysis. A total of 129 differentially expressed genes (49 up-regulated; 80 down-regulated) were found, considering a 1.5-fold change and a 16% FDR (Supplemental Table S1). qRT-PCR analysis was used to validate expression of the nonmodulated NRAS, ROCK1, PI3KCA, COPZ1, GRB2, and CXCL5 and of the differentially expressed DYRK2, CSF1, CTSA, ITGA5, MMP15, and NRP1 (not shown). By crossing these results with putative miR-148b targets (TargetScan 5.1), 20 common genes (19 down-regulated; 1 up-regulated) were found (**Fig. 4***A*), among them ITGA5, known to modulate apoptosis, adhesion, migration, and invasion (29, 30), and CSF1, involved in tumor-stroma interactions (31, 32). Using TargetScan predictions for an IPA, GM-CSF and integrin pathways were identified as statistically significant (Supplemental Fig. S3). Therefore, we investigated the plausible direct regulation of these pathways by miR-148b and their involvement in breast tumor progression. Protein expression was evaluated for ITGA5 and its downstream players ROCK1, PI3KCA/p110α, and NRAS (predicted targets) and for CSF1 in miR-148b-overexpressing MDAMB231 or 4175TGL cells by Western blot analysis. Strong reductions were found compared to controls (Fig. 4*B*). Instead, when miR-148b was down-modulated in MCF7 cells, increased levels of ITGA5 proteins were observed (Fig. 4*B*). Interestingly, ROCK1, PI3KCA/p110α, and NRAS were not modulated at the mRNA level (not shown). Direct modulation of miR-148b on its targets was proven by performing luciferase assays in miR-148b-overexpressing or control MDAMB231 cells transfected with reporter vectors containing wild-type or mutated 3′-UTRs (Fig. 4*C*, *D*). As positive control, a miR-148b-sensor construct was used (Fig. 4*C*). Notably, when we evaluated miR-148b target expression on a subset of relapsing/nonrelapsing human tumors, differential expression was found (**Fig. 5***A*). Relevantly, when the 23 predicted and modulated miR-148b target genes were used in IPA to look for gene connections, cell-to-cell signaling and interaction, tissue development, cellular movement network was identified (Ingenuity score=22; Fig. 5*B*). Given the relevance of the integrin pathway in our investigations, we evaluated the possibility that the upstream player ITGA5 can be used to predict survival in a large microarray dataset of human breast tumors (26). Performing hierarchical clustering and Kaplan-Meier analyses and referring to

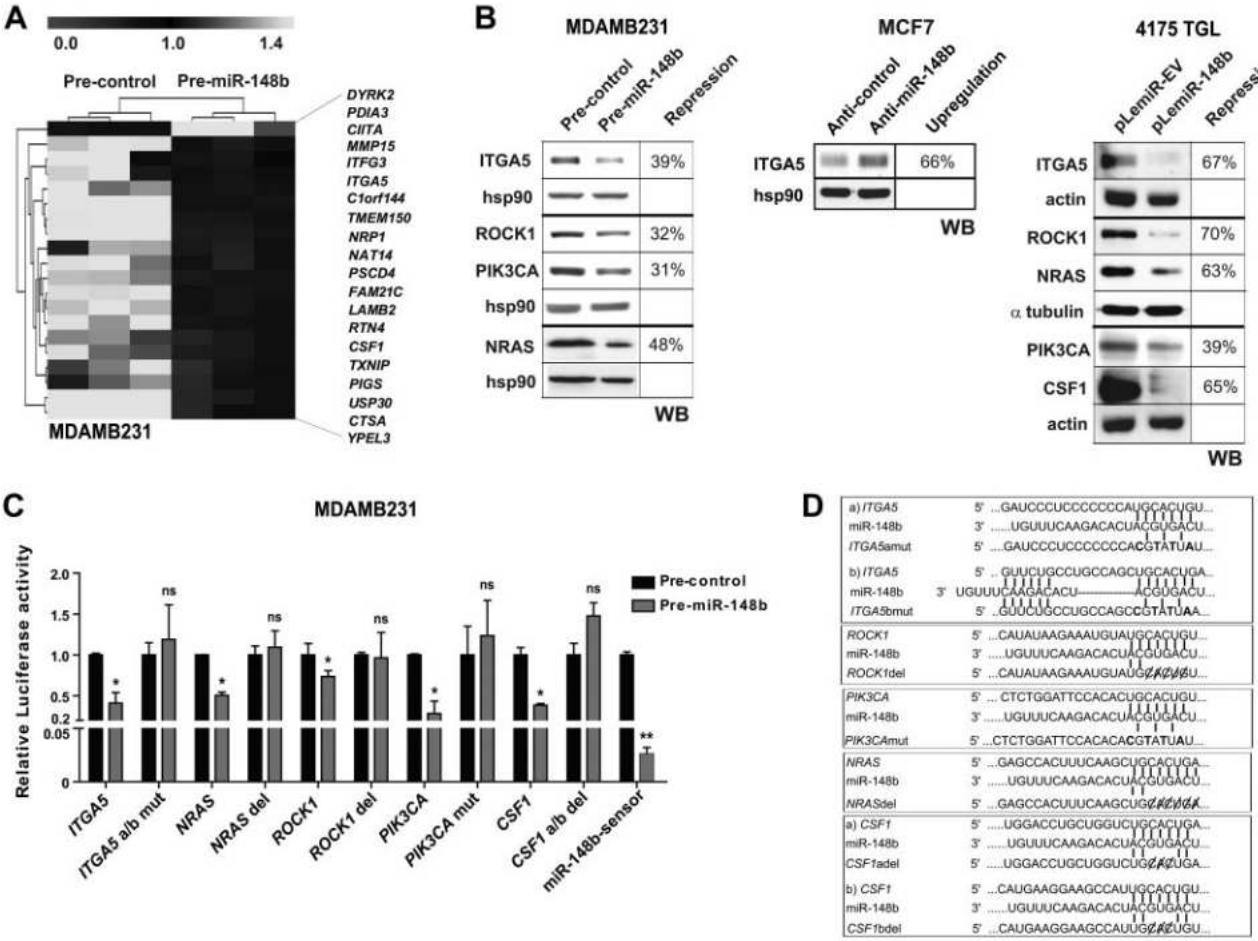

Figure 4. miR-148b modulates multiple genes. MDAMB231 or MCF7 cells transfected with miR-148b precursors or inhibitors or their negative controls (pre- and anti-miR-148b or pre- and anti-control) analyzed at 48 or 72 h post-transfection or 4175TGL cells stably transduced with pLemiR-EV or pLemiR-148b overexpression vectors were used to perform microarray analysis (*A*), Western blots (*B*), or luciferase assays (*C*). *A*) Clustering (Pearson correlation, average linkage) was performed for 20 putative miR-148b targets. Heatmap represents relative gene expression with reference to the median across all samples; row: protein-coding gene; column: cell preparation. *B*) Western blot (WB) analysis was performed for 5 putative miR-148b targets: ITGA5, ROCK1, p110α (PIK3CA), NRAS, and CSF1. Protein expression was calculated relative to controls, following miR-148b overexpression or down-modulation, normalized on the indicated loading controls (hsp90/actin/αtubulin) and expressed as repression percentages. *C*, *D*) Luciferase assays (*C*) in cells transfected with reporter constructs containing wild-type or mutant 3′-UTRs (*D*) for the indicated genes or a synthetic sequence including 3 perfect miR-148b binding sites (sensor). Results are shown as means ± SEM of firefly luciferase activity relative to controls, normalized on *Renilla* luciferase activity. mut, mutation; del, deletion; a/b, a and b binding sites; ns, not significant. Three independent experiments were performed with independent protein (WB and luciferase) or RNA preparations. Representative results are shown in *B*; results are pooled in *C*. $^*P < 0.05$; $^{**}P < 0.01$.

ITGA5 median expression, we predicted DFS (Fig. 5*C*). This, together with similar results reported previously (33), suggests that repression of ITGA5 correlates with better clinical outcome and can be used as a prognostic marker.

Down-modulation of ITGA5 accounts for miR-148b chemotherapy response

The effect of integrin signaling on cell survival and chemotherapy response was evaluated in the absence of serum and adhesion (anoikis) or in presence of paclitaxel. When ITGA5 was silenced with siRNAs in MDAMB231 cells, reduction in cell survival was observed in anoikis conditions and for paclitaxel-treated cells *vs.* controls (**Fig. 6***A*). Instead, when ITGA5 (cDNA lacking its 3′-UTR) was overexpressed (pEGFP-ITGA5), together with pre-miR-148b, in MDAMB231 or MCF7 cells (Fig. 6*B*), and with cells kept in the presence of paclitaxel, the effect of miR-148b on cell death was abolished (Fig. 3). Figure 6*B* considers only the difference (Δ) observed when comparing the presence or absence of miR-148b. ITGA5 and miR-148b levels were evaluated by qRT-PCR analysis (Fig. 6*C–E*). From these results, we can conclude that ITGA5 directly controls, at least partially, miR-148b-driven apoptosis in anoikis conditions and in the presence of paclitaxel.

DISCUSSION

In this work, we identified a group of 16 miRs that are associated with bad prognosis in our breast cancer

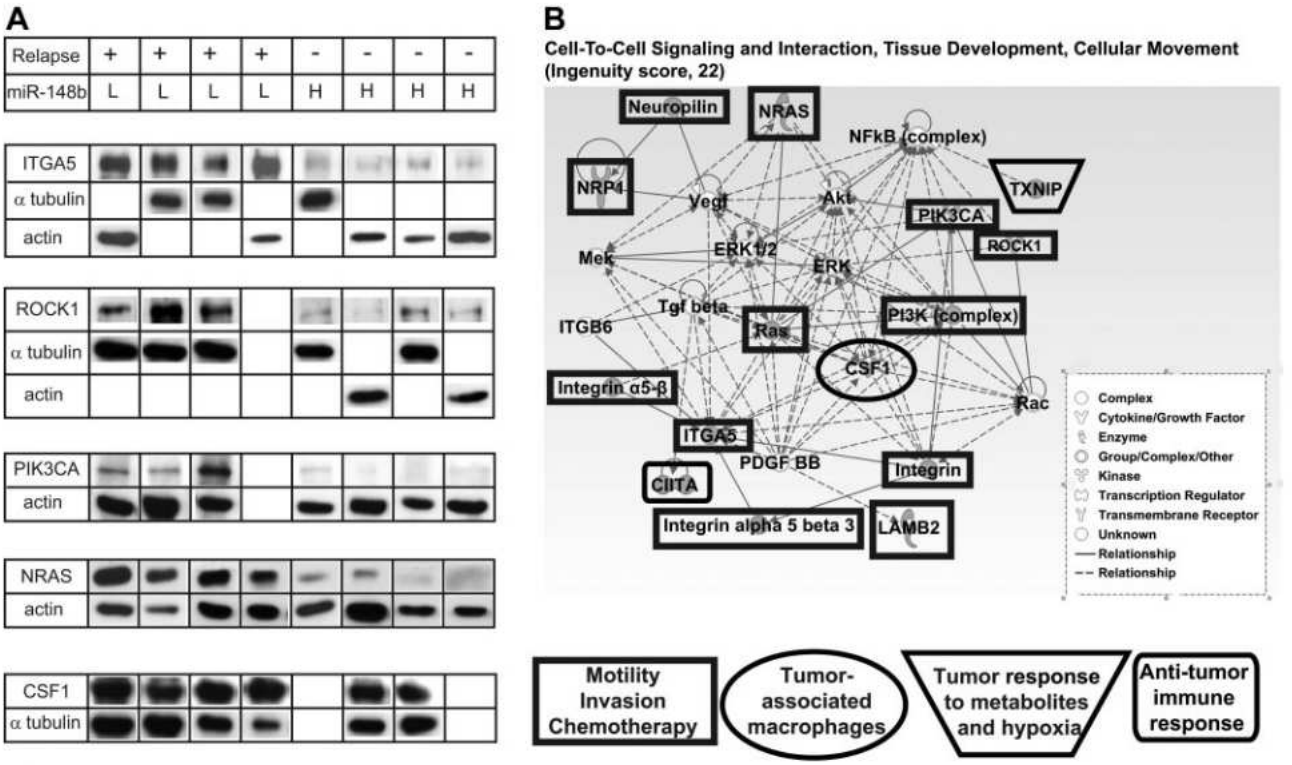

Figure 5. Analysis of miR-148b-modulated genes in human tumors and by IPA. *A*) Proteins were extracted from relapsing or nonrelapsing primary breast tumors, and Western blot (WB) analysis was performed for the direct miR-148b targets, ITGA5, ROCK1, PIK3CA, NRAS, and CSF1. miR-148b expression is indicated as low (L) or high (H), according to previous microarray and/or qRT-PCR analyses. α-Tubulin or actin was used as loading control. *B*) Twenty miR-148b down-modulated genes identified in the microarray analysis (Fig. 4*A*) plus the 3 direct targets, ROCK1, PIK3CA, and NRAS, were used to perform an IPA searching for gene connections; the cell-to-cell signaling and interaction, tissue development, cellular movement functional network was generated. Ingenuity score: $-\log_{10} P = 22$. Gene products are represented as nodes and biological relationships between two nodes as a line. Continuous lines indicate direct interactions; dashed lines represent indirect connections. Shapes of nodes symbolize functional classes of gene products (see legend in panel). Gray symbols indicate down-regulation; white symbols indicate genes absent in the input but related with the dataset used. *C*) Kaplan-Meier analyses of the probability of DFS of breast cancer patients based on ITGA5 expression (median) in Wang *et al.* (26) dataset for 286 breast tumor samples. *P* value was calculated using the log-rank test.

patient cohort, and we revealed the function of miR-148b as a metastasis suppressor in mice, as well as its molecular mechanism of action. The identification of a group of miRs that could identify primary tumor subtypes is highly relevant for the clinics. In fact, it represents a potent molecular tool that clinicians can use at the time of surgery to attempt the most appropriate therapy for every patient. The strength of this tool is further marked by the fact that single components of the signature, for instance miR-148b, can predict tumor outcome individually. Relevantly, low levels of miR-148b were observed previously in basal-like (9) and $ERBB2^+/ER^-/PR^-$ (34) breast tumors, which suggests its involvement in malignancy.

Our functional experiments with metastatic cells strongly suggest that miR-148b exerts its metastasis-suppressing role mostly by controlling cell movement. In fact, while it is true that ectopic expression of miR-148b in malignant tumor cells leads to decreased tumor growth, this effect is modest and not sufficient to justify the much more pronounced control of metastasis dissemination. On this line, increased miR-148b levels lead to stronger adhesion and anoikis and reduce invasion *in vitro*. Moreover, *in vivo*, miR-148b strongly reduces extravasation and lung colonization shortly after injection of the cells in the blood circulation, when proliferation has no time to play a major role. Overall, it is well accepted that miRs have pleiotropic functions and therefore can act in independent events, such as tumor formation and progression, *via* the activation/repression of a selective and rate-limiting cascade of specific genes (8, 35–37).

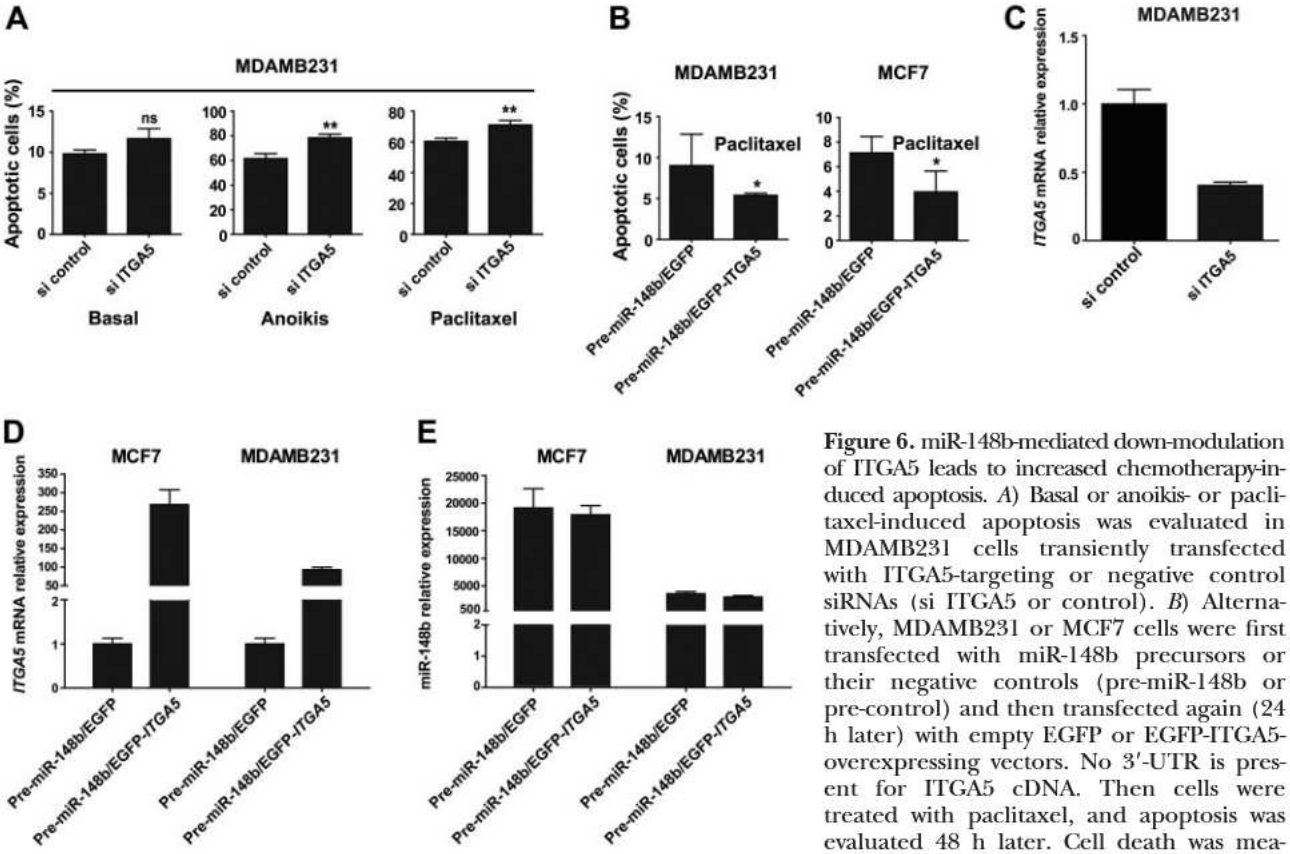

Figure 6. miR-148b-mediated down-modulation of ITGA5 leads to increased chemotherapy-induced apoptosis. *A*) Basal or anoikis- or paclitaxel-induced apoptosis was evaluated in MDAMB231 cells transiently transfected with ITGA5-targeting or negative control siRNAs (si ITGA5 or control). *B*) Alternatively, MDAMB231 or MCF7 cells were first transfected with miR-148b precursors or their negative controls (pre-miR-148b or pre-control) and then transfected again (24 h later) with empty EGFP or EGFP-ITGA5-overexpressing vectors. No 3′-UTR is present for ITGA5 cDNA. Then cells were treated with paclitaxel, and apoptosis was evaluated 48 h later. Cell death was measured by TMRM and annexinV-FITC (*A*) or AnnexinV-PE stainings (*B*) by FACS analysis. *A*) ^{High}TMRM-^{Low}AnnexinV, healthy cells; ^{Low}TMRM-^{High}AnnexinV, apoptotic cells. *B*) ^{Low}AnnexinV, healthy cells; ^{High}AnnexinV, apoptotic cells. Two or 3 independent experiments were performed in duplicate; pooled quantitations are shown as means ± SD. *C–E*) qRT-PCR analyses were performed to evaluate ITGA5 mRNA or miR-148b expression for the cells shown in *A* and *B*. Two independent experiments were performed in triplicate, and a representative one is shown. ns, not significant. $*P < 0.05$; $**P < 0.01$.

Among all the miR-148b-modulated genes identified in this study, many are known to be relevant in tumor progression, among them, CTSA, NRP1, CSF1, MMP15, and ITGA5, all suppressed by miR-148b. By focusing on the ITGA5 signaling, we found that not only ITGA5 but also ROCK1, PIK3CA/p110α, and NRAS are directly down-regulated by miR-148b, which suggests a specific control for this miR on a pathway known to be involved in metastasis dissemination and chemotherapy response. In fact, ITGA5 and ROCK1 were found previously to be highly expressed in malignant breast tumors and are known to increase tumor growth or progression (33, 38–42). At the same time, PIK3CA/p110α is relevant for mammary tumorigenesis and angiogenesis (43), as well as for resistance to endocrine or anti-HER2 therapies (44, 45). In addition, NRAS is a well-known oncogene, and its silencing in tumor cells leads to increased apoptosis (46). Regarding chemotherapy response, elevated levels and activity of α5β1 have previously been implicated in drug resistance (47), and inhibition of α5β1/fibronectin interactions promotes apoptosis in malignant cells and enhances radiation effects (33). In addition, perturbations of the actin cytoskeleton integrity *via* ROCK1 inhibition commit cells to apoptosis (48). Remarkably, ITGA5 and its downstream player RHOA, a ROCK activator, have been previously found to be suppressed by miR-31, another small noncoding RNA that suppresses metastasis (36). In addition, ROCK1 and RHOC are also directly targeted by two other miRs involved in tumor progression, miR-146a/b and miR-10b (49, 50). The fact that CSF1 is also a direct target of miR-148b opens up a role for this small RNA in tumor-stroma cell interactions, which will be part of a future study. In summary, our study unravels the association of a group of 16 miRs with bad prognosis tumors and identifies miR-148b as a suppressor of tumor progression and modulator of chemotherapy response acting *via* the integrin. FJ

This work was supported by grants from the University of Torino (Local Research Funding, 2007 and 2008; D.T.), Compagnia-San-Paolo (2008.1054; D.T.), Programma di Ricerca di Rilevante Interesse Nazionale (PRIN; 2008; D.T. and PRIN 2009; M.D.B.), Associazione Italiana Ricerca Cancro (AIRC; 2008-IG-6014, G.L.; 2009-IG-9408, P.P.; 2010-IG-10104; D.T.), and Fondo per gli Investimenti della Ricerca di Base (FIRB-giovani2008, RBFR08F2FS-002; F.O.). F.O. and D.C. were fellows of the Regione Piemonte. The authors thank P.P. Pandolfi for helpful discussions; V. Poli and E. Hirsch for critical reading of the manuscript; J. Massaguè (Memorial Sloan-Kettering Cancer Center, New York, NY, USA) and L. Primo and P. Circosta (University of Torino, Turin, Italy) for providing cell lines; A. R. Elia for the FACS analysis; A. Mana for performing

some experiments; L. Fuso, G. M. Milano, F. Maggiorotto, and C. Robba for the patient datasets; and A. F. Horwitz (University of Illinois, Urbana-Champaign, IL, USA, *via* Addgene, Cambridge, MA, USA) for the 15238 plasmid. The authors declare no conflicts of interest.

REFERENCES

1. Liu, S., Clouthier, S. G., and Wicha, M. S. Role of microRNAs in the regulation of breast cancer stem cells. *J. Mammary Gland Biol. Neoplasia* **17,** 15–21
2. Dunnwald, L. K., Rossing, M. A., and Li, C. I. (2007) Hormone receptor status, tumor characteristics, and prognosis: a prospective cohort of breast cancer patients. *Breast Cancer Res.* **9,** R6
3. Colozza, M., Cardoso, F., Sotiriou, C., Larsimont, D., and Piccart, M. J. (2005) Bringing molecular prognosis and prediction to the clinic. *Clin. Breast Cancer* **6,** 61–76
4. Sorlie, T., Perou, C. M., Tibshirani, R., Aas, T., Geisler, S., Johnsen, H., Hastie, T., Eisen, M. B., van de Rijn, M., Jeffrey, S. S., Thorsen, T., Quist, H., Matese, J. C., Brown, P. O., Botstein, D., Eystein Lonning, P., and Borresen-Dale, A. L. (2001) Gene expression patterns of breast carcinomas distinguish tumor subclasses with clinical implications. *Proc. Natl. Acad. Sci. U. S. A.* **98,** 10869–10874
5. Sotiriou, C., and Piccart, M. J. (2007) Taking gene-expression profiling to the clinic: when will molecular signatures become relevant to patient care? *Nat. Rev. Cancer* **7,** 545–553
6. Bartel, D. P. (2009) MicroRNAs: target recognition and regulatory functions. *Cell* **136,** 215–233
7. Lu, J., Getz, G., Miska, E. A., Alvarez-Saavedra, E., Lamb, J., Peck, D., Sweet-Cordero, A., Ebert, B. L., Mak, R. H., Ferrando, A. A., Downing, J. R., Jacks, T., Horvitz, H. R., and Golub, T. R. (2005) MicroRNA expression profiles classify human cancers. *Nature* **435,** 834–838
8. Blenkiron, C., Goldstein, L. D., Thorne, N. P., Spiteri, I., Chin, S. F., Dunning, M. J., Barbosa-Morais, N. L., Teschendorff, A. E., Green, A. R., Ellis, I. O., Tavare, S., Caldas, C., and Miska, E. A. (2007) MicroRNA expression profiling of human breast cancer identifies new markers of tumor subtype. *Genome Biol.* **8,** R214
9. Enerly, E., Steinfeld, I., Kleivi, K., Leivonen, S. K., Aure, M. R., Russnes, H. G., Ronneberg, J. A., Johnsen, H., Navon, R., Rodland, E., Makela, R., Naume, B., Perala, M., Kallioniemi, O., Kristensen, V. N., Yakhini, Z., and Borresen-Dale, A. L. miRNA-mRNA integrated analysis reveals roles for miRNAs in primary breast tumors. *PLoS One* **6,** e16915
10. Shi, M., Liu, D., Duan, H., Shen, B., and Guo, N. Metastasis-related miRNAs, active players in breast cancer invasion, and metastasis. *Cancer Metastasis Rev.* **29,** 785–799
11. Le, X. F., Merchant, O., Bast, R. C., and Calin, G. A. The roles of MicroRNAs in the cancer invasion-metastasis cascade. *Cancer Microenviron.* **3,** 137–147
12. Penna, E., Orso, F., Cimino, D., Tenaglia, E., Lembo, A., Quaglino, E., Poliseno, L., Haimovic, A., Osella-Abate, S., De Pitta, C., Pinatel, E., Stadler, M. B., Provero, P., Bernengo, M. G., Osman, I., and Taverna, D. microRNA-214 contributes to melanoma tumour progression through suppression of TFAP2C. *EMBO J.* **30,** 1990–2007
13. Minn, A. J., Kang, Y., Serganova, I., Gupta, G. P., Giri, D. D., Doubrovin, M., Ponomarev, V., Gerald, W. L., Blasberg, R., and Massague, J. (2005) Distinct organ-specific metastatic potential of individual breast cancer cells and primary tumors. *J. Clin. Invest.* **115,** 44–55
14. Simpson, J. F., Gray, R., Dressler, L. G., Cobau, C. D., Falkson, C. I., Gilchrist, K. W., Pandya, K. J., Page, D. L., and Robert, N. J. (2000) Prognostic value of histologic grade and proliferative activity in axillary node-positive breast cancer: results from the Eastern Cooperative Oncology Group Companion Study, EST 4189. *J. Clin. Oncol.* **18,** 2059–2069
15. Tarone, G., Russo, M. A., Hirsch, E., Odorisio, T., Altruda, F., Silengo, L., and Siracusa, G. (1993) Expression of beta 1 integrin complexes on the surface of unfertilized mouse oocyte. *Development* **117,** 1369–1375
16. Laukaitis, C. M., Webb, D. J., Donais, K., and Horwitz, A. F. (2001) Differential dynamics of alpha 5 integrin, paxillin, and alpha-actinin during formation and disassembly of adhesions in migrating cells. *J. Cell Biol.* **153,** 1427–1440
17. Wang, X., Tian, W., and Li, Y. (2008) Development of an efficient protocol of RNA isolation from recalcitrant tree tissues. *Mol. Biotechnol.* **38,** 57–64
18. Bolstad, B. M., Irizarry, R. A., Astrand, M., and Speed, T. P. (2003) A comparison of normalization methods for high density oligonucleotide array data based on variance and bias. *Bioinformatics* **19,** 185–193
19. Risso, D., Massa, M. S., Chiogna, M., and Romualdi, C. (2009) A modified LOESS normalization applied to microRNA arrays: a comparative evaluation. *Bioinformatics* **25,** 2685–2691
20. Tibshirani, R., Hastie, T., Narasimhan, B., and Chu, G. (2002) Diagnosis of multiple cancer types by shrunken centroids of gene expression. *Proc. Natl. Acad. Sci. U. S. A.* **99,** 6567–6572
21. Saeed, A. I., Bhagabati, N. K., Braisted, J. C., Liang, W., Sharov, V., Howe, E. A., Li, J., Thiagarajan, M., White, J. A., and Quackenbush, J. (2006) TM4 microarray software suite. *Methods Enzymol.* **411,** 134–193
22. Liu, Y. (2008) Box plots: use and interpretation. *Transfusion* **48,** 2279–2280
23. Zweig, M. H., and Campbell, G. (1993) Receiver-operating characteristic (ROC) plots: a fundamental evaluation tool in clinical medicine. *Clin. Chem.* **39,** 561–577
24. Mantel, N. (1966) Evaluation of survival data and two new rank order statistics arising in its consideration. *Cancer Chemother. Rep.* **50,** 163–170
25. Gill, R. (1982) Understanding Cox's regression model. *Exper. Suppl.* **41,** 187–199
26. Wang, Y., Klijn, J. G., Zhang, Y., Sieuwerts, A. M., Look, M. P., Yang, F., Talantov, D., Timmermans, M., Meijer-van Gelder, M. E., Yu, J., Jatkoe, T., Berns, E. M., Atkins, D., and Foekens, J. A. (2005) Gene-expression profiles to predict distant metastasis of lymph-node-negative primary breast cancer. *Lancet* **365,** 671–679
27. Damasco, C., Lembo, A., Somma, M. P., Gatti, M., Di Cunto, F., and Provero, P. A signature inferred from Drosophila mitotic genes predicts survival of breast cancer patients. *PLoS One* **6,** e14737
28. Lewis, B. P., Burge, C. B., and Bartel, D. P. (2005) Conserved seed pairing, often flanked by adenosines, indicates that thousands of human genes are microRNA targets. *Cell* **120,** 15–20
29. Mierke, C. T., Frey, B., Fellner, M., Herrmann, M., and Fabry, B. Integrin alpha5beta1 facilitates cancer cell invasion through enhanced contractile forces. *J. Cell Sci.* **124,** 369–383
30. Desgrosellier, J. S., and Cheresh, D. A. Integrins in cancer: biological implications and therapeutic opportunities. *Nat. Rev. Cancer* **10,** 9–22
31. Abraham, D., Zins, K., Sioud, M., Lucas, T., Schafer, R., Stanley, E. R., and Aharinejad, S. Stromal cell-derived CSF-1 blockade prolongs xenograft survival of CSF-1-negative neuroblastoma. *Int. J. Cancer* **126,** 1339–1352
32. Aharinejad, S., Paulus, P., Sioud, M., Hofmann, M., Zins, K., Schafer, R., Stanley, E. R., and Abraham, D. (2004) Colony-stimulating factor-1 blockade by antisense oligonucleotides and small interfering RNAs suppresses growth of human mammary tumor xenografts in mice. *Cancer Res.* **64,** 5378–5384
33. Nam, J. M., Chung, Y., Hsu, H. C., and Park, C. C. (2009) beta1 integrin targeting to enhance radiation therapy. *Int. J. Radiat. Biol.* **85,** 923–928
34. Mattie, M. D., Benz, C. C., Bowers, J., Sensinger, K., Wong, L., Scott, G. K., Fedele, V., Ginzinger, D., Getts, R., and Haqq, C. (2006) Optimized high-throughput microRNA expression profiling provides novel biomarker assessment of clinical prostate and breast cancer biopsies. *Mol. Cancer* **5,** 24
35. Ma, L., and Weinberg, R. A. (2008) Micromanagers of malignancy: role of microRNAs in regulating metastasis. *Trends Genet.* **24,** 448–456
36. Valastyan, S., Chang, A., Benaich, N., Reinhardt, F., and Weinberg, R. A. Concurrent suppression of integrin alpha5, radixin, and RhoA phenocopies the effects of miR-31 on metastasis. *Cancer Res.* **70,** 5147–5154
37. Tavazoie, S. F., Alarcon, C., Oskarsson, T., Padua, D., Wang, Q., Bos, P. D., Gerald, W. L., and Massague, J. (2008) Endogenous human microRNAs that suppress breast cancer metastasis. *Nature* **451,** 147–152

38. Valastyan, S., Benaich, N., Chang, A., Reinhardt, F., and Weinberg, R. A. (2009) Concomitant suppression of three target genes can explain the impact of a microRNA on metastasis. *Genes Dev.* **23,** 2592–2597
39. Taverna, D., and Hynes, R. O. (2001) Reduced blood vessel formation and tumor growth in alpha5-integrin-negative teratocarcinomas and embryoid bodies. *Cancer Res.* **61,** 5255–5261
40. Liu, S., Goldstein, R. H., Scepansky, E. M., and Rosenblatt, M. (2009) Inhibition of rho-associated kinase signaling prevents breast cancer metastasis to human bone. *Cancer Res.* **69,** 8742–8751
41. Lane, J., Martin, T. A., Watkins, G., Mansel, R. E., and Jiang, W. G. (2008) The expression and prognostic value of ROCK I and ROCK II and their role in human breast cancer. *Int. J. Oncol.* **33,** 585–593
42. Zheng, B., Liang, L., Wang, C., Huang, S., Cao, X., Zha, R., Liu, L., Jia, D., Tian, Q., Wu, J., Ye, Y. W., Wang, Q., Long, Z., Zhou, Y., Du, C., He, X., and Shi, Y. MicroRNA-148a suppresses tumor cell invasion and metastasis by downregulating ROCK1 in gastric cancer. *Clin. Cancer Res.* **17,** 7574–7583
43. Renner, O., Blanco-Aparicio, C., Grassow, M., Canamero, M., Leal, J. F., and Carnero, A. (2008) Activation of phosphatidylinositol 3-kinase by membrane localization of p110alpha predisposes mammary glands to neoplastic transformation. *Cancer Res.* **68,** 9643–9653
44. Eichhorn, P. J., Gili, M., Scaltriti, M., Serra, V., Guzman, M., Nijkamp, W., Beijersbergen, R. L., Valero, V., Seoane, J., Bernards, R., and Baselga, J. (2008) Phosphatidylinositol 3-kinase hyperactivation results in lapatinib resistance that is reversed by the mTOR/phosphatidylinositol 3-kinase inhibitor NVP-BEZ235. *Cancer Res.* **68,** 9221–9230
45. Miller, T. W., Hennessy, B. T., Gonzalez-Angulo, A. M., Fox, E. M., Mills, G. B., Chen, H., Higham, C., Garcia-Echeverriav C., Shyr, Y., and Arteaga, C. L. Hyperactivation of phosphatidylinositol-3 kinase promotes escape from hormone dependence in estrogen receptor-positive human breast cancer. *J. Clin. Invest.* **120,** 2406–2413
46. Eskandarpour, M., Kiaii, S., Zhu, C., Castro, J., Sakko, A. J., and Hansson, J. (2005) Suppression of oncogenic NRAS by RNA interference induces apoptosis of human melanoma cells. *Int. J. Cancer* **115,** 65–73
47. Nista, A., Leonetti, C., Bernardini, G., Mattioni, M., and Santoni, A. (1997) Functional role of alpha4beta1 and alpha5beta1 integrin fibronectin receptors expressed on adriamycin-resistant MCF-7 human mammary carcinoma cells. *Int. J. Cancer* **72,** 133–141
48. Shi, J., and Wei, L. (2007) Rho kinase in the regulation of cell death and survival. *Arch. Immunol. Ther. Exp. (Warsz.)* **55,** 61–75
49. Lin, S. L., Chiang, A., Chang, D., and Ying, S. Y. (2008) Loss of mir-146a function in hormone-refractory prostate cancer. *RNA* **14,** 417–424
50. Ma, L., Teruya-Feldstein, J., and Weinberg, R. A. (2007) Tumour invasion and metastasis initiated by microRNA-10b in breast cancer. *Nature* **449,** 682–688

Received for publication July 25, 2012.
Accepted for publication November 13, 2012.